SLAS Discovery
2017, Vol. 22(6) 686–695

DOI: 10.1177/2472555217696794
journals.sagepub.com/home/jbx
SAGE

High-Throughput Patch Clamp Screening in Human α6-Containing Nicotinic Acetylcholine Receptors

Lucas C. Armstrong[1], Glenn E. Kirsch[1], Nikolai B. Fedorov[1], Caiyun Wu[1], Yuri A. Kuryshev[1], Abby L. Sewell[1], Zhiqi Liu[1], Arianne L. Motter[2], Carmine S. Leggett[2], and Michael S. Orr[2*]

Abstract

Nicotine, the addictive component of tobacco products, is an agonist at nicotinic acetylcholine receptors (nAChRs) in the brain. The subtypes of nAChR are defined by their α- and β-subunit composition. The α6β2β3 nAChR subtype is expressed in terminals of dopaminergic neurons that project to the nucleus accumbens and striatum and modulate dopamine release in brain regions involved in nicotine addiction. Although subtype-dependent selectivity of nicotine is well documented, subtype-selective profiles of other tobacco product constituents are largely unknown and could be essential for understanding the addiction-related neurological effects of tobacco products. We describe the development and validation of a recombinant cell line expressing human $\alpha6/3\beta2\beta3^{V273S}$ nAChR for screening and profiling assays in an automated patch clamp platform (IonWorks Barracuda). The cell line was pharmacologically characterized by subtype-selective and nonselective reference agonists, pore blockers, and competitive antagonists. Agonist and antagonist effects detected by the automated patch clamp approach were comparable to those obtained by conventional electrophysiological assays. A pilot screen of a library of Food and Drug Administration–approved drugs identified compounds, previously not known to modulate nAChRs, which selectively inhibited the $\alpha6/3\beta2\beta3^{V273S}$ subtype. These assays provide new tools for screening and subtype-selective profiling of compounds that act at α6β2β3 nicotinic receptors.

Keywords

nicotinic acetylcholine receptor, automated patch clamp, electrophysiological screening, ion channel

Introduction

Nicotine, the addictive component of tobacco products, derives its physiological effects by mimicking acetylcholine (ACh), a neurotransmitter that acts at ionotropic nicotinic acetylcholine receptors (nAChRs) broadly distributed in the central and peripheral nervous systems.[1,2] nAChRs are pentameric ligand-gated, cation-permeable ion channels that depolarize neuronal membranes. In the brain, nAChRs on presynaptic terminals modulate neurotransmitter release, and postsynaptic nAChRs depolarize neuronal membranes and can produce a calcium influx sufficient for activation of second messenger systems. Central nervous system (CNS) and peripheral nervous system–specific nAChR subtypes are defined primarily by their α- and β-subunit composition, which determines their pharmacological characteristics, including their selectivity to specific agonists and antagonists, as well as their biophysical properties such as Ca^{2+} ion permeability and response kinetics. A nicotinic cholinergic component has been identified in several neurological conditions as well as tobacco addiction. For instance, α4β2 and α7 subtypes are widely distributed in the brain and have been investigated on the basis of interest in tobacco addiction and cognitive deficit, respectively.[3,4] By contrast, α6* (where * denotes the inclusion of additional subunits) has a more restricted distribution, primarily in retina and catecholaminergic nuclei (e.g., locus coeruleus, substantia

[1]Charles River Discovery, Cleveland, OH, USA
[2]U.S. Food and Drug Administration/Center for Tobacco Products, Silver Spring, MD, USA
*Current affiliation: PAREXEL International, Bethesda, MD, USA

Received Mar 23, 2016, and in revised form Jan 24, 2017, Accepted for publication Jan 25, 2017.

Supplementary material is available online with this article.

Corresponding Author:
Lucas C. Armstrong, Charles River Discovery, 14656 Neo Parkway, Cleveland, OH 44128, USA.
Email: luke.armstrong@crl.com

nigra, and ventral tegmental area). The α6β2β3 nAChR subtype, in particular, is expressed in terminals of dopaminergic neurons that project to the nucleus accumbens and striatum, where it modulates dopamine release in brain regions involved in nicotine addiction.[5,6]

Despite its emerging physiological significance, α6* receptors have been difficult targets to investigate as compared with other nAChR subtypes, in part because of poor in vitro performance in heterologous expression systems.[7] This limitation has been partially overcome by molecular engineering of the receptor proteins to create chimeric and/or mutated subunits with improved functional expression in cells. In particular, cell lines were previously created containing a chimeric α6/α3 subunit in which the α6 extracellular N-terminal domain (a major determinant of ACh binding) is linked to the transmembrane and C-terminal domains of the α3 subunit (including pore-lining segment).[8,9] When cotransfected with cDNAs encoding β2 and $\beta3^{V273S}$ (valine to serine mutation cRNAs, located in the pore-lining region of β3, that promotes function), the resulting $\alpha6/\alpha3\beta2\beta3^{V273S}$ receptor generated ionic current in response to ACh, which could be inhibited by α-conotoxin MII (a selective competitive antagonist of native α6β2* receptors).[8,10] Thus, $\alpha6/\alpha3\beta2\beta3^{V273S}$ recapitulates the native α6β2β3 function in regard to the ligand-binding site. However, high-throughput patch clamp techniques suitable for screening and profiling have not yet been applied to the engineered α6* receptors. Our laboratory has previously demonstrated the utility of the automated electrophysiology platform, IonWorks Barracuda, for high-throughput analysis of the nAChR subtypes α3β4, α3β4α5, α4β2, and α7.[11] In the present study, we demonstrate the suitability of this high-throughput electrophysiological assay for screening and selectively profiling the human $\alpha6/3\beta2\beta3^{V273S}$ nAChR receptor.

Methods

Cloning of cDNAs into a Mammalian Expression Vector

Plasmids containing cDNAs for human CHRNA6, CHRNB2, and CHRNB3 were obtained from OriGene Technologies (Rockville, MD). The plasmid encoding human CHRNA3 was amplified by PCR from pooled cDNA from the spinal cord and retina. The full-length cDNAs for CHRNB2 and CHRNB3 were PCR amplified to be modified with an optimized translation initiation sequence. CHRNB3 was cloned into pcDNA3.1 with G418 resistance, and CHRNB2 was cloned into pcDNA3.1-hygro by standard molecular biology methods. The CHRNB3 sequence was subjected to site-directed mutagenesis to change the codon encoding the amino acid at position 273 from valine to serine. To construct the chimeric CHRNA6/CHRNA3 cDNA, the 5′ segment of CHRNA6 and 3′ segment of CHRNA3 were amplified by PCR and ligated into pcDNA3.1-puro. Resulting plasmids were sequenced at the Cleveland Clinic Foundation core facility (Cleveland, OH), and the sequences were compiled and compared with reference sequences. The translated sequence of the CHRNB2 cDNA was determined to be identical to that of GenBank accession number NM_000748. The translated sequence of the CHRNB3 cDNA was determined to be identical to that of GenBank accession number NM_000749, with the aforementioned V273S mutation. The translated sequence of the chimeric CHRNA6/CHRNA3 cDNA was found to be identical to amino acids 1 to 237 in the translated GenBank accession number NM_004198, directly followed by amino acids 239 to 505 in the translated GenBank accession number NM_000743.

Several other nicotinic subtypes (α3β4, α3β4α5, α4β2, and α7) were expressed in recombinant cell lines and used in selectivity profiling experiments. These cell lines were developed previously in our lab.[11]

Transfection of HEK Cells

Transfection-ready cDNAs were linearized in nonessential regions of the plasmid to facilitate incorporation into the host cell genomic DNA. HEK 293 host cells (American Type Culture Collection, Manassas, VA) were grown in DMEM/F12 media supplemented with 10% fetal bovine serum, glutamine, and penicillin/streptomycin in a 37 °C incubator at 5% CO_2 and 95% humidity. Cell density was limited to 70% to 80% confluence by passing cells at least twice a week. Cells were detached with Accutase (Innovative Cell Technologies, San Diego, CA) and neutralized in media, then centrifuged and resuspended in Nucleofection buffer. Linearized plasmid DNA constructs were mixed gently with cells and transferred into cuvettes for electroporation (Nucleofector, Lonza America Inc., Allendale, NJ). Electroporated cells were allowed to recover in media and then transferred into 60 mm dishes with complete medium lacking selection antibiotics. Medium containing selection antibiotics (G418, hygromycin, and puromycin) was added 24 to 48 h posttransfection and refreshed twice a week until colonies were apparent.

Selection of Clones Stably Expressing α6/3, β2, and β3

After 2 to 3 wk of antibiotics selection, surviving cells were detached, suspended, and sorted by FACSAria (BD Biosciences, San Jose, CA) as single cells into 96-well plates. Clones were propagated and screened for functional activity in IonWorks Barracuda (IWB, Molecular Devices, LLC, Sunnyvale, CA) to determine expression level and homogeneity. The top three positive clones (B4, B14, and G5) were cryopreserved in liquid nitrogen and analyzed by Western blot for

subunit ratios and quantities. Two clones (B4 and G5) with appropriate ratios of proteins were characterized by reverse transcriptase PCR (RT-PCR; **Suppl. Fig. S1**) to determine mRNA ratios, as described below. B4 and G5 clones were expanded, and master cell banks were cryopreserved.

RT-PCR Procedures. Total RNA was isolated from ~1 × 10^6 cells using Qiagen RNeasy Mini Kit (Qiagen, Inc., Valencia, CA). The RNA concentration was measured by ultraviolet scan and also examined on 1% agarose gel.

The cellular RNA was diluted in RNase-free water to 2 µg/40 µL. Complementary DNA was synthesized from the cellular RNA with a Clontech Sprint RT Complete-Double PrePrimed cDNA synthesis kit (Clontech Laboratories, Inc., Mountain View, CA). Cellular RNA not subjected to reverse transcriptase was used as a template control for the RT-PCR reaction.

Cellular cDNA, cellular RNA (negative control), and positive control plasmid cDNAs were subjected to PCR amplification subunit-specific oligonucleotides, and the PCR products were analyzed on a 1% agarose gel.

Western Blot Procedures. Total cell lysates were prepared from α6/3β2β3^{V273S} nAChR clones in cold RIPA buffer and clarified by centrifugation at 10,000 × *g*. Proteins were separated by sodium dodecyl sulfate–polyacrylamide gel electrophoresis using NuPAGE 4%~12% Bis-Tris gel (Life Technologies, Grand Island, NY), blotted onto polyvinylidene difluoride membranes, and blocked with 5% nonfat dry milk in Tris-buffered saline with Tween 20 (TTBS). Blots were incubated with primary antibodies against α3 (ab110801, Abcam, Cambridge, MA) and β2 (sc-1449, Santa Cruz Biotechnology, Inc., Dallas, TX) in milk overnight. Blots were washed in TTBS and incubated with secondary antibody for 1 h at room temperature. The blots were developed with the ECL Plus detection system and exposed to X-ray film.

Electrophysiological Procedures

Cell-Handling Procedures. To prepare for electrophysiological experiments, cells were routinely maintained in growth media containing the appropriate selection of antibiotics, as described above. On the day before the assay, the cells were refed with medium lacking selection antibiotics and moved to a 27 °C incubator with 5% CO_2 and 95% humidity, a treatment that has been demonstrated to increase trafficking of ion channels to the cell surface.[12] Cell density was ~50% to 70% confluent at the time of harvest; two 150 mm plates (approximately 1.2 × 10^7 cells) were used per population patch clamp (PPC) experiment. Alternatively, cells were harvested, resuspended in cryopreservation media at 10% DMSO, and aliquoted in vials for use as assay-ready cells after thawing from cryogenic storage.

Cultured cells were harvested by washing twice with 15 to 20 mL of Hank's Balanced Salt Solution (HBSS) lacking calcium and magnesium and treatment with 5 mL of Accutase solution for 20 min. Cells were resuspended in a 50 mL conical tube with addition of 10 mL of HBSS and triturated with a serological pipette to resuspend the cells and break up cell clusters. Alternatively, frozen assay-ready cells were thawed rapidly in a 37 °C water bath, transferred to a 50 mL conical tube, resuspended in growth media (DMEM/F12-PS/10% fetal bovine serum), and centrifuged at ~250 × *g* for 5 min. The medium was aspirated and replaced with 10 mL fresh media to remove DMSO.

Cells were triturated, transferred to a 50 mL conical tube, and pelleted at 500 × *g* for 2.5 min. The supernatant was removed and the cell pellet was resuspended in 10 mL of HBSS. The cell suspension was centrifuged again at 500 × *g* for 2.5 min, and the supernatant was removed. Finally, the cell pellet was resuspended in 5 mL of HEPES-buffered physiological saline, and the cells were dispensed to the assay plate.

Solutions and Reagents. Chemicals used in solution preparation were purchased from Sigma-Aldrich (St. Louis, MO) and were of ACS reagent grade purity or higher. Stock solutions of test articles were prepared in DMSO and stored frozen. Each test article formulation was sonicated (model 2510/5510, Branson Ultrasonics, Danbury, CT) at ambient room temperature for 20 min to facilitate dissolution. Test article concentrations were prepared fresh daily by diluting stock solutions into extracellular solution (HBPS buffer). The solution composition was 137 mM NaCl, 4 mM KCl, 4 mM $CaCl_2$, 1 mM $MgCl_2$, 10 mM HEPES, and 10 mM glucose, pH adjusted to 7.4 with NaOH. All test and control solutions contained 0.3% DMSO. The test article formulations were prepared in 384-well compound plates using an automated liquid-handling system (Sciclone, PerkinElmer, Waltham, MA). The internal HEPES-buffered solution consisted of 90 mM CsF, 50 mM CsCl, 2 mM $MgCl_2$, 5 mM EGTA, and 10 mM HEPES, pH 7.2 adjusted with CsOH. Stock solution of escin was prepared in DMSO (14 mg/mL) and added to the solution at the final concentration of 14 µg/mL to achieve patch perforation in the whole-cell recording mode. Extracellular buffer was loaded into the PPC plate wells (11 µL per well), and cell suspension was added into the wells (9 µL per well). After establishment of a whole-cell configuration (10 min escin perforation), membrane currents were recorded by on-board patch clamp amplifiers in IonWorks Barracuda. The data acquisition frequency was 5 kHz. Inward current amplitudes and charge movement (area under the curve) were measured. Under these conditions, each assay was completed in 45 min, and 5 to 10 experiments could be conducted each 8-h day.

Ionic currents were elicited with application of 20 µL agonist (10 µL/s). Antagonists were added 5 min before

EC_{90} (-)-nicotine application. To evaluate effects of positive modulators, currents were elicited with EC_{20} (-)-nicotine. Recordings were started 2 s before the application, with a total recording duration of 17 s. The holding potential was −70 mV.

Food and Drug Administration–Approved Drug Library

A library of 786 Food and Drug Administration (FDA)–approved drugs was purchased from Enzo Life Sciences (Screen-Well compound library, BML-2843-0100). Compounds were received as 100 µL samples dissolved mainly in DMSO (except for one compound in water) at 10 mM. Daughter plates were prepared in 384-well format, and compounds were screened at a final concentration of 2 µM. The potency of selected compounds was measured at concentrations up to 20 µM. Screening and potency confirmation experiments were conducted in an agonist/antagonist modulator mode by preincubation with test compound for 2 min followed by challenge with test compound plus ligand (nicotine) at ~EC_{90} concentration.

Data Analysis

Data acquisition and analyses were performed using the IWB system software (version 2.0.0.335, Molecular Devices Corporation, Sunnyvale, CA). Data were corrected for leak current. Offline data analysis was performed in Microsoft Excel.

Activation Calculation. nAChR activation was calculated as:

$$\%\ \text{Activation} = \left(I_{agon} / I_{Max}\right) \times 100\%$$

where I_{agon} was the agonist-elicited current and I_{Max} was the mean current elicited with a high concentration of (-)-nicotine (as specified in the text).

Concentration-response data were fitted to an equation of the form:

$$\%\ \text{Activation} = \%\ \text{VC} + \left\{\frac{\left(\%\ \text{MAX} - \%\ \text{VC}\right) /}{\left[1 + \left([\text{Test}] / EC_{50}\right)^{N}\right]}\right\}$$

where [Test] was the concentration of agonist, EC_{50} was the concentration of agonist producing half-maximal activation, N is the Hill coefficient, % VC was the percentage of current fluctuation at addition (the mean current at the DMSO vehicle control addition), % MAX is the percentage of the current activated with the highest dose of (-)-nicotine, and % Activation is the percentage of the current elicited at each concentration of agonist. Nonlinear least-squares fits were solved with the XLfit add-in for Excel 2003 (Microsoft, Redmond, WA).

Inhibition calculation. Inhibitory effects were calculated as:

$$\%\ \text{Block} = \left(1 - I_{TA} / I_{Control}\right) \times 100\%$$

where I_{TA} was the (-)-nicotine-elicited current in the presence of a test article and $I_{Control}$ was the mean (-)-nicotine EC_{90} -elicited current.

Antagonist concentration-response data were fit to an equation of the following form:

$$\%\ \text{Change} = \%\ \text{Min} + \left\{\frac{\left(\%\ \text{Max} - \%\ \text{Min}\right) /}{\left[1 + \left([\text{Test}] / IC_{50}\right)^{N}\right]}\right\}$$

where [Test] was the concentration of a test article, IC_{50} was the concentration of the test article producing half-maximal inhibition, N is the Hill coefficient, % Min was the mean current elicited with (-)-nicotine EC_{90} plus vehicle control, % Min was the current measured at the DMSO vehicle addition, and % Block was the percentage of the current inhibited at each concentration of a test compound.

Acceptance Criteria. Individual well data were filtered, and experiments were accepted according to the criteria listed in Table 1.

The Z′ factor in each experiment was calculated as

$$Z' = 1 - \left(3 \times \text{SDVC} + 3 \times \text{SDPC}\right) / \text{ABS}\left(\text{MeanVC} - \text{MeanPC}\right)$$

where MeanVC and SDVC were the mean and standard deviation values for a vehicle control and MeanPC and SDPC are the mean and standard deviation values for a positive control.

Results

Expression confirmation

Expression of the nicotinic receptor subunit message was evaluated as depicted in **Supplementary Figure S1A**. RT-PCR was performed with primer sets specific for each subunit, CHRNA6, CHRNA3, CHRNB2, and CHRNB3 in candidate α6/3β2β3 nAChR clones. Clones B4 and G5 but not untransfected HEK 293 expressed mRNAs encoding the chimera of α6/3, β3, β2, and $\beta3^{V273S}$ subunits. Both clones B4 and G5 expressed similar amounts of the mRNAs encoding α6/3 and β2. However, clone G5 appeared to express a slightly higher amount of the mRNA encoding β3 than clone B4.

Confirmation of protein expression by immunoblotting assay was performed as shown in **Supplementary Figure S1B**. Lysates of α6/3β2β3 candidate clones B4, B14, and G5 and untransfected HEK 293 cells were analyzed by

Table 1. Acceptance criteria.

Parameter	Acceptance Criterion
PPC well level	
R_{SEAL} (baseline)[a]	>100 MΩ
Current amplitude (baseline)	>0.1 nA
R_{SEAL} stability (between first and second additions)	<50% decrease
PPC plate level	
Z′ factor	≥0.4
Success rate (% valid wells)	>90% accepted wells per PPC plate
EC/IC_{50} for reference compounds	≤0.5 log from historical mean

PPC = population patch clamp.
[a]Typical R_{seal} values ranged between 200 and 1000 MΩ.

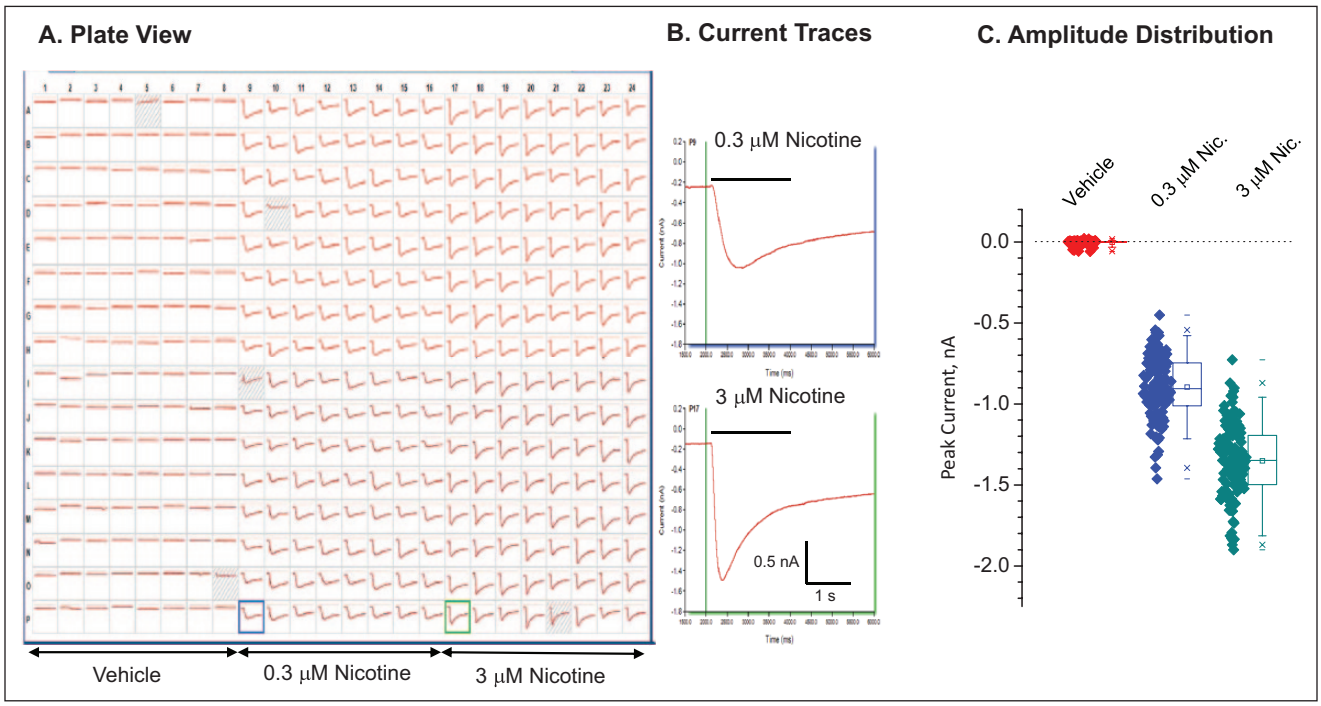

Figure 1. Functional expression in IonWorks Barracuda. Cells were thawed from cryogenic storage and dispensed into the assay plate in population patch clamp mode. (**A**) Current traces in plate view. (**B**) Sample records at higher magnification. The vertical line indicates application of ligand. The receptors were activated by application of either 0.3 or 3 μM (-)-nicotine. (**C**) Amplitude distribution. Holding potential, –70 mV. Mean seal resistance ± SD = 422.5 ± 84 MΩ (n = 380 wells). Four wells were invalid (<100 MΩ, shaded wells).

Western blotting with antibodies against the α3 and β2 nicotinic ACh receptor subunits (an antibody capable of β3 detection was not available for these experiments). The results demonstrate expression of α3 and β2 proteins in the candidate α6/3β2β3 nAChR clones. The α3 and β2 antibodies each detected bands of ~57 kD in the candidate α6/3β2β3 clones. These molecular weights correspond to the predicted molecular weights of 57 kD. The bands were not present in the untransfected HEK 293 cells. The immunoblotting results confirmed the expression of the α6/3 and β2 subunits in the HEK293 cells for each of the candidate α6/3β2β3 nAChR clones. Clone G5 appeared to express the highest levels of protein and was selected for functional confirmation.

Functional Characterization in Automated Patch Clamp

Functional characterization was performed in IonWorks Barracuda automated patch clamp (**Fig. 1**). Receptor activation by 0.3 and 3 μM (-)-nicotine at holding potential, –70 mV, evoked a concentration-dependent inward current that

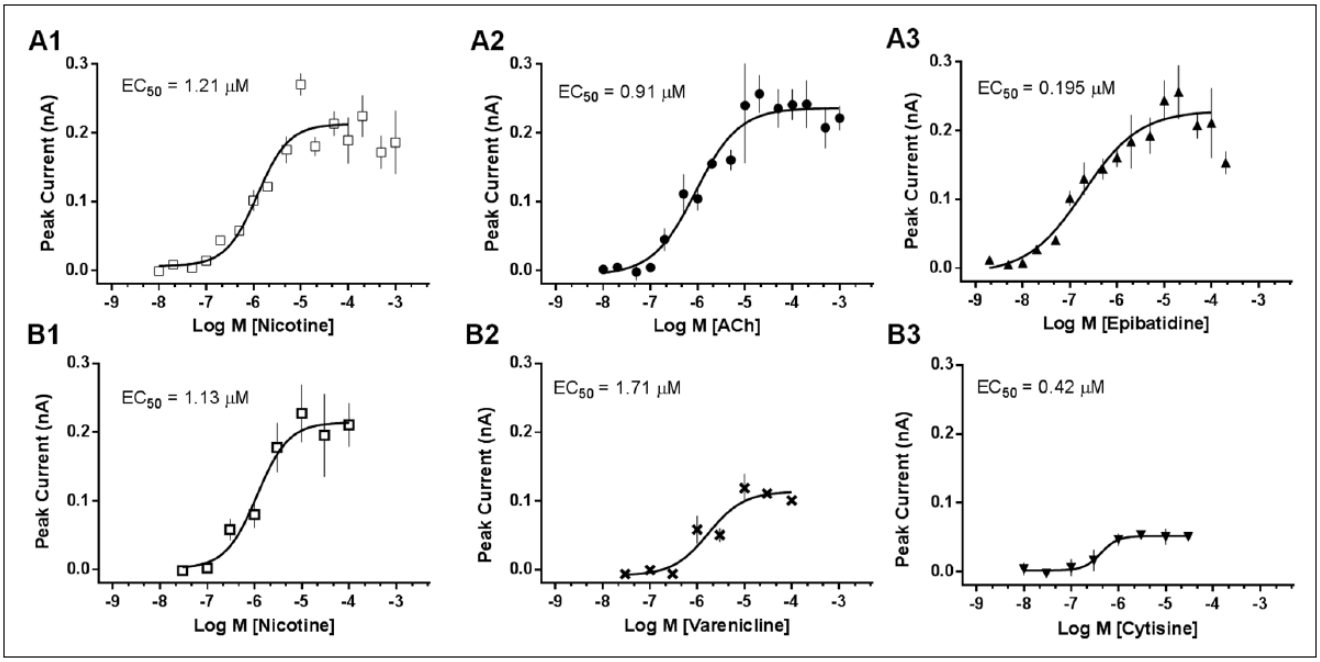

Figure 2. Agonist assay validation. (**A**) Concentration-response curves (16-point) were obtained for three full agonists in two independent experiments on different days. Compounds were administered at the indicated concentrations, and responses were recorded simultaneously. (**B**) Concentration-response curves (eight-point) for partial agonists, varenicline and cytisine. Data points represent mean peak current ± SEM (two to four replicate wells/concentration). Curves were fitted to the data by a one-site model.

displayed an initial rapid decay followed by a slower decay over the 3-s recording period. The biphasic decay of current in the continued presence of ligand is thought to represent the slowed desensitization introduced by the V273S mutation in β3.[10]

The potency of nicotine to stimulate currents and the tolerance for the presence of DMSO in the external solution was evaluated as shown in **Supplementary Figure S2**. The ionic currents showed concentration-dependent activation with average EC_{50} values of 0.73, 0.88, and 3.69 μM, respectively, in the presence of 0%, 0.5%, and 2.5% DMSO. We selected 0.3% DMSO as a standard concentration for preparing dosing solutions in subsequent experiments.

We characterized the potencies of reference agonists as shown in **Figure 2**. Agonists, nicotine, ACh, and epibatidine, were evaluated in 16-point concentration-response format (**Fig. 2**, A1–A3). Application of the ligands elicited concentration-dependent activation of inward ionic currents. Activation was calculated from the peak current amplitude and plotted versus $\log_{10}$[ligand]. The rank order of potency based on EC_{50} values (**Table 2**) was epibatidine > nicotine ≈ ACh. The nicotine and ACh values compare favorably with published data.[10]

Partial agonists, varenicline and cytisine, were evaluated in eight-point concentration-response format and compared with the full agonist, nicotine (**Fig. 2**, B1–B3). At maximum concentration (100 μM) varenicline and cystisine, respectively, showed 51% and 32% efficacy relative to nicotine. The rank order of potency based on EC_{50} values was cytisine (0.4 μM) > nicotine (1.1 μM) > varenicline (2.1 μM).

Antagonist validation (**Fig. 3**) included the noncompetitive antagonists mecamylamine, bupropion, and SR 16584[13–16] and competitive antagonist dihydro-β-erythroidine.[17] The rank order of potency based on IC_{50} values was mecamylamine ≈ dihydro-β-erythroidine > bupropion > SR 16584.

Profiling of a Registered Drug Library

We tested the feasibility of using the assay as a tool for identifying nicotine subtype-selective modulators by conducting a pilot evaluation of the Enzo ScreenWell library of 786 FDA-registered drugs (Enzo Life Sciences, Inc., Farmingdale, NY) against $\alpha6/3\beta2\beta3^{V273S}$. Compounds were preincubated at 2 μM for 5 min and then challenged with (-)-nicotine at the EC_{90} concentration of 3 μM. Recordings obtained during preincubation showed no evidence of agonist effects, apart from the expected effects of known agonists (e.g., varenicline, ACh, and nicotine). In contrast, some of the recordings obtained during nicotine challenge gave evidence of strong inhibitory effects, several of which were generated by known inhibitors and a few of which were generated by novel inhibitors. We defined "active" inhibitors as compounds that decreased peak current by at least 65% relative to the average response in the vehicle control wells after nicotine challenge, which represents

Table 2. Potency of agonists in concentration-response curves on α6/α3β2β3^{V273S}.

	EC_{50}, μM (Confidence Interval)				
Reference Agonist	Day 1	Day 2	Average	Published	Ref.
Acetylcholine	0.91 (0.43–1.95)	0.92 (0.41–2.09)	0.915	0.94	10
(-)-Nicotine	1.21 (0.78–1.86)	0.42 (0.23–0.76)	0.815	0.14	10
Epibatidine	0.20 (0.076–0.50)	0.08 (0.023–0.28)	0.14	0.1	8

approximately 5% of the compounds in the library. We confirmed 33 actives from the 786 compounds tested and then evaluated the selectivity of the 33 actives in a concentration-response format. Subtype selectivity profiling was performed in five human nicotinic subtypes: α3β4, α3β4α5, α4β2, α6/3β2β3^{V273S}, and α7.

Figure 4 shows the IC_{50} profiles of seven of the most potent compounds. In addition to known nAChR inhibitors (bupropion, imipramine, pancuronium, mecamylamine, and methyllycaconitine), actives included two compounds, epinastine and pentamidine, which showed subtype-selective effects not previously associated with nicotinic receptor inhibition. The α6/3β2β3^{V273S} subtype was the most sensitive subtype to inhibition by epinastine with an IC_{50} value of 0.528 ± 0.098 μM, whereas the other four nAChR subtypes displayed IC_{50} values ≥1 μM. Pentamidine inhibited the α7 and α6/3β2β3^{V273S} subtypes most potently, with IC_{50} values of 0.152 ± 0.017 and 0.522 ± 0.021 μM, respectively.

Discussion

Nicotinic receptors that contain the α6β2β3 subunits are of particular interest because of nonclinical evidence of their involvement in nicotine addiction[6] and because of their potential relevance in neurological diseases.[5] The native α6β2β3 nAChR subtype is expressed in terminals of dopaminergic neurons that project to the nucleus accumbens and striatum. In vivo studies with α6 knockout mice and ex vivo brain slice studies employing toxins selectively inhibiting α6-containing nAChRs demonstrate that such α6-expressing neurons modulate dopamine release in brain regions involved in nicotine addiction.[5,6] Thus, they could play a key role in CNS function and present a reasonable target for research on tobacco and tobacco-related products that contain both nicotine and additional ingredients, of which may modify nicotine's action at the receptor level.

However, pharmacological studies have been hampered by difficulties in generating sufficient levels of functional expression of α6β2β3 nAChR in heterologous systems, including both *Xenopus* oocytes and mammalian cells. Kuryatov et al[7] demonstrated that a chimeric construct consisting of the extracellular domain of α6 and the intracellular domain of α3 or α4 when coexpressed with β2 and β3 resulted in functional receptors in *Xenopus* oocytes. More recently, Capelli et al[8] showed that transfection of human embryonic kidney (HEK 293) cells with cDNAs encoding the human α6/3 chimera, β2, and β3^{V273S} subunits gave useable levels of functional channels suitable for pharmacological experiments. Therefore, we adopted the approach of engineering a chimeric α6/3β2β3^{V273S} and stably transfecting HEK 293 cells. It is important to note that the composite structure of the chimeric α6/3 subunit, consisting of the α6 extracellular N-terminal domain (major determinant of ACh binding) linked to the transmembrane and C-terminal domains of the α3 subunit (including a pore-lining segment), would be expected to have an orthosteric ligand-binding site with properties that resemble those of native α6β2* but with sensitivity to pore blockers that more closely resembles that of α3-containing receptor subtypes.

In the present study, we demonstrated for the first time the suitability of a high-throughput electrophysiological assay for screening and selectivity profiling of the human α6/3β2β3^{V273S} nAChR receptor in HEK 293 cells. Our results showed that the α6/3β2β3^{V273S}-HEK cell line exhibits appropriate molecular and functional characteristics to enable high-throughput (384-well) automated assays in PPC format.

RT-PCR results showed that the CHRNB2, CHRNB3, and chimeric CHRNA6/CHRNA3 mRNAs were expressed accurately in clones of the α6/3β2β3^{V273S}-HEK cell line. Western blotting analysis demonstrated that both the α6/3 and β2 proteins with correct molecular weights were robustly expressed in candidate clones.

Electrophysiological analysis of the α6/3β2β3^{V273S}-HEK cell line in IonWorks showed that the cell line has the appropriate response to nicotine and sufficient expression uniformity to serve as a test system for pharmacological assays designed to quantify sensitivity to agonists and antagonists. Experimental conditions were optimized for sensitivity and reproducibility by recording in the cell population mode (PPC) and by adjusting the positive control agonist and DMSO concentrations. We evaluated the assay tolerance for DMSO at concentrations of 0%, 0.5%, 1.5%, and 2.5%, and at 0.5% DMSO, we observed acceptable Z′ values (a statistical measure of assay quality that includes both variability and signal dynamic range) 0.50 to 0.53, indicative of a robust assay.

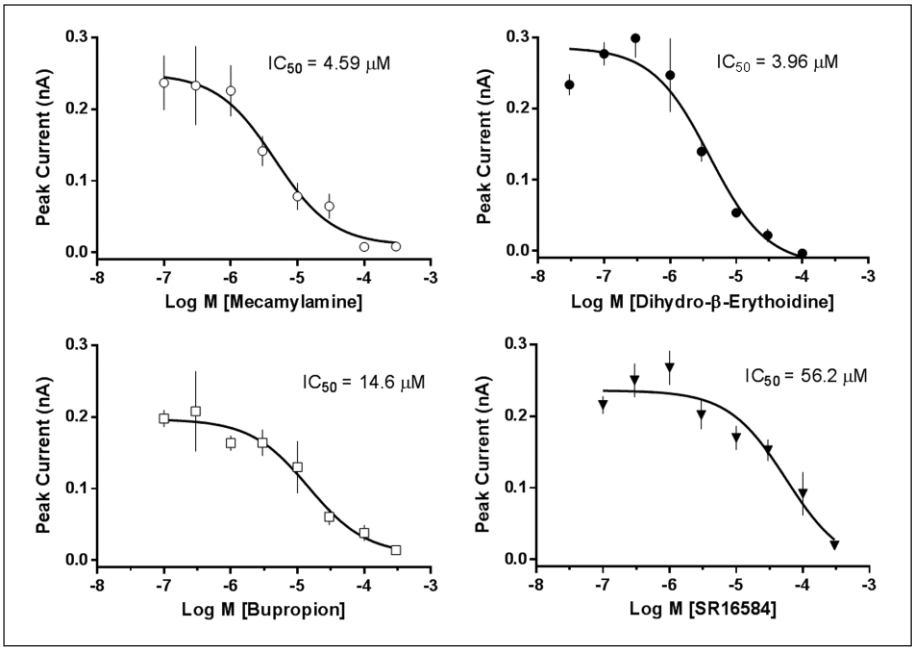

Figure 3. Antagonist mode validation. Concentration-response curves (eight-point) were obtained for reference antagonists in two independent experiments on different days. Cells were preincubated with test compound at the indicated concentrations. Cells were stimulated with (-)-nicotine at a supramaximal concentration (30 µM). Data points represent mean peak current ± SEM (three to four replicate wells/concentration).

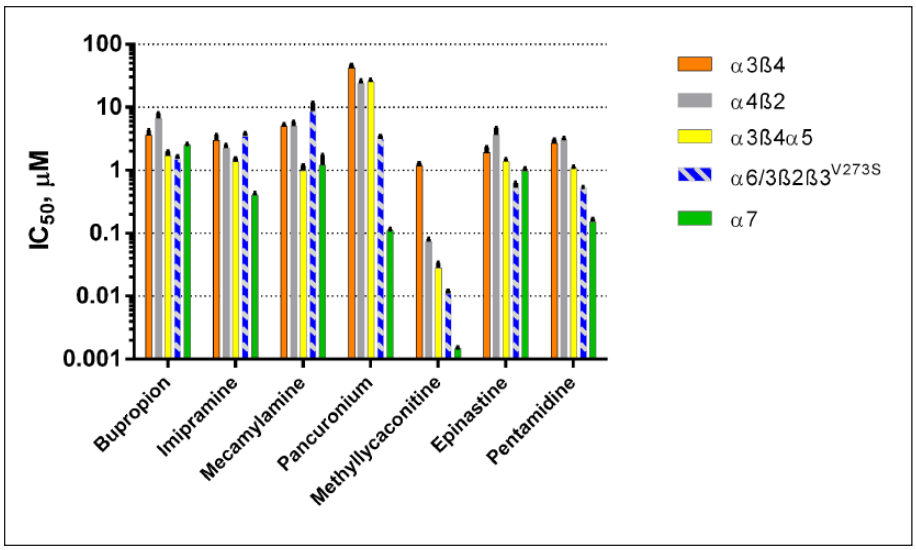

Figure 4. Subtype profiling of known and novel nicotinic acetylcholine receptors inhibitors. Mean IC_{50} values ± SEM (n = 2–4) obtained in four-point (0.02–20 µM) or eight-point (methyllycaconitine only, 0.001–3 µM) concentration-response curves. The cells were preincubated with the test compounds for 2 min and then stimulated with (-)-nicotine at EC_{90} concentrations (100 µM for α3β4, α4β2, and α3β4α5; 3 µM for $\alpha6/3\beta2\beta3^{V273S}$; and 3 µM + 1 µM PNU 120596 for α7).

We showed that this test system was capable of reproducing reference compound pharmacology similar to that reported in the literature from patch clamp and fluorescence assay studies.[10] As expected, $\alpha6/3\beta2\beta3^{V273S}$ showed high sensitivity to plant-derived nicotine, animal-derived epibatidine, and the natural ligand, ACh. In our assays, all three substances exhibited full agonist activity. By contrast, the synthetic compound varenicline and the related, plant-derived cytisine behaved as partial agonists in line with the known characteristics of these compounds on $\alpha6/3\beta2\beta3^{V273S}$.[10] Antagonist validation included mecamylamine, dihydro-β-erythroidine, bupropion, SR 16584, and methyllycaconitine. The rank order of potency based on IC_{50} values was methyllycaconitine >> mecamylamine ≈ dihydro-β-erythroidine > bupropion >> SR 16584 (α3β4-selective), consistent with previous reports from analysis by manual patch clamp and fluorescence assays.[8,10,16]

We evaluated the effects of 786 FDA-registered drugs in the Enzo ScreenWell library as a test of the ability of the system to identify agonists or antagonists in screening mode. In single-point screening, we successfully detected known nicotinic agonists including nicotine, ACh, and varenicline, but novel agonists were not identified in this screen. From known antagonists that were detected in the initial screen, we selected five compounds for additional receptor subtype profiling. These included four from the

Enzo library of drugs (bupropion, imipramine, mecamylamine, and pancuronium) and methyllycaconitine, a positive control. This group included both competitive inhibitors acting at the orthosteric ligand-binding site and noncompetitive inhibitors acting at allosteric sites to modulate receptor activity by one or more mechanisms such as voltage-dependent pore blockade and channel gating modulation. Methyllycaconitine[18] and pancuronium[19] act as competitive inhibitors that displace agonists and show decreased affinity at elevated agonist concentrations. By contrast, noncompetitive inhibitors, which exhibit potencies independent of agonist concentration, are thought to act by a variety of mechanisms including open-channel (e.g., mecamylamine), closed-channel (e.g., imipramine), or channel state–independent blockade (e.g., bupropion).[20,21]

Based on preservation of the α6β2β3 ligand-binding site in the α6/3β2β3^{V273S} construct, we hypothesized that competitive inhibitors would show the greatest degree of selectivity compared with the other subtypes, whereas noncompetitive inhibitors would show little selectivity between α6/3β2β3^{V273S} and related receptor subtypes that included α3 (i.e., α3β4 and α3β4α5) or β2 (i.e., α4β2) subunits. This expectation was supported by results that showed that bupropion and imipramine, antidepressants with known nicotinic receptor inhibitory effects, and mecamylamine, an antihypertensive ganglionic blocker, were relatively nonselective between the receptor subtypes. Compared with α3β4, α3β4α5, and α4β2, however, α6/3β2β3^{V273S} showed higher sensitivity to the muscle relaxant pancuronium and to the positive control, methyllycaconitine. Moreover, for these two compounds, α6/3β2β3^{V273S} showed much less sensitivity than the unrelated α7 subtype.

In addition to known inhibitors, the group of 33 actives included two compounds, epinastine and pentamidine, with novel subtype-selective effects not previously reported. In selectivity profiling experiments, these compounds showed submicromolar potency against α6/3β2β3^{V273S} and modest levels of selectivity. Although not previously identified as a nicotinic receptor antagonist, epinastine, an anti-allergenic drug that acts as a histamine H1 receptor antagonist, has been shown to inhibit voltage-gated potassium channels[22] and N-type calcium channels[23] at micromolar concentrations. Also, pentamidine, an anti-infective drug, shows evidence of ion channel modulating activity, including potent inhibition of ionotropic NMDA glutamate receptors[24] and proton-activated ASIC channels.[25]

Compared with related subtypes (α3β4, α3β4α5, and α4β2), α6/3β2β3^{V273S} showed selectivity for epinastine ranging from 6.9-fold greater potency versus α4β2 to 2.6-fold versus α3β4α5. Similarly, pentamidine was selective for α6/3β2β3^{V273S} by a ratio of 5.8-fold versus α4β2 to 2.0-fold versus α3β4α5. This pattern of selectivity is consistent with activity against the orthosteric ligand-binding site on α6/3β2β3^{V273S}, but additional work would be necessary to establish a competitive mechanism of action. By contrast, compared with the unrelated α7 subtype, α6/3β2β3^{V273S} showed little selectivity, 1.9-fold and 0.3-fold, respectively, for epinastine and pentamidine.

It is interesting that in patients, epinastine plasma levels (C_{max}) can reach ~0.1 μM,[26] well within range of the α6/3β2β3^{V273S} concentration-response (epinastine IC_{50} = 0.5 μM). However, epinastine crosses the blood-brain barrier with efficiency of only ~10%, lessening the significance for generating CNS side effects.[27] Similarly, pentamidine can reach micromolar plasma concentrations (~1.8 μM),[28] but its efficiency in crossing the blood-brain barrier is quite low (~0.04%),[29] making CNS side effects via α6/3β2β3^{V273S} (IC_{50} = 0.52 μM) or α7 (IC_{50} = 0.15 μM) unlikely.

In conclusion, our validation experiments with reference compounds demonstrated the capability of the test system for evaluating concentration-dependent α6/3β2β3^{V273S} modulation in a functional, 384-well patch clamp platform. Moreover, the capability of the assay to identify potent, subtype-selective inhibitors was verified in pilot library screening and profiling experiments. Therefore, we suggest that the high-throughput automated patch clamp tool described in this investigation will be a valuable method for evaluation of nicotinic subtype selectivity. This investigative tool advances tobacco regulatory science as it provides a rapid screening method to identify tobacco product constituents that act at α6β2β3 nicotinic receptors.

Declaration of Conflicting Interests

The authors declared no potential conflicts of interest with respect to the research, authorship, and/or publication of this article.

Funding

The authors acknowledge funding from the United States Food and Drug Administration HHSF223201510026C and HHSF223201310070C.

References

1. Dani, J. A.; Heinemann, S. Molecular and Cellular Aspects of Nicotine Abuse. *Neuron* **1996**, *16*, 905–908.
2. Tuesta, L. M.; Fowler, C. D.; Kenny, P. J. Recent Advances in Understanding Nicotinic Receptor Signaling Mechanisms That Regulate Drug Self-Administration Behavior. *Biochem. Pharmacol*. **2011**, *82*, 984–995.
3. Coe, J. W.; Brooks, P. R.; Vetelino, M. G.; et al. Varenicline: An Alpha4beta2 Nicotinic Receptor Partial Agonist for Smoking Cessation. *J. Med. Chem*. **2005**, *48*, 3474–3477.
4. Wallace, T. L.; Porter, R. H. Targeting the Nicotinic Alpha7 Acetylcholine Receptor to Enhance Cognition in Disease. *Biochem. Pharmacol*. **2011**, *82*, 891–903.
5. Quik, M.; Perez, X. A.; Grady, S. R. Role of Alpha6 Nicotinic Receptors in CNS Dopaminergic Function: Relevance to Addiction and Neurological Disorders. *Biochem. Pharmacol*. **2011**, *82*, 873–882.
6. Brunzell, D. H. Preclinical Evidence That Activation of Mesolimbic Alpha 6 Subunit Containing Nicotinic Acetylcholine Receptors Supports Nicotine Addiction Phenotype. *Nicotine Tob. Res*. **2012**, *14*, 1258–1269.

7. Kuryatov, A.; Olale, F.; Cooper, J.; et al. Human Alpha6 AChR Subtypes: Subunit Composition, Assembly, and Pharmacological Responses. *Neuropharmacology* **2000**, *39*, 2570–2590.
8. Capelli, A. M.; Castelletti, L.; Chen, Y. H.; et al. Stable Expression and Functional Characterization of a Human Nicotinic Acetylcholine Receptor with Alpha6beta2 Properties: Discovery of Selective Antagonists. *Br. J. Pharmacol.* **2011**, *163*, 313–329.
9. Dowell, C.; Olivera, B. M.; Garrett, J. E.; et al. Alpha-Conotoxin PIA Is Selective for Alpha6 Subunit-Containing Nicotinic Acetylcholine Receptors. *J. Neurosci*. **2003**, *23*, 8445–8452.
10. Rasmussen, A. H.; Strobaek, D.; Dyhring, T.; et al. Biophysical and Pharmacological Characterization of Alpha6-Containing Nicotinic Acetylcholine Receptors Expressed in HEK293 Cells. *Brain Res*. **2014**, *1542*, 1–11.
11. Kirsch, G. E.; Fedorov, N. B.; Kuryshev, Y. A.; et al. Electrophysiology-Based Assays to Detect Subtype-Selective Modulation of Human Nicotinic Acetylcholine Receptors. *Assay Drug Dev. Technol*. **2016**, *14*, 333–344.
12. Chen, M. X.; Sandow, S. L.; Doceul, V.; et al. Improved Functional Expression of Recombinant Human Ether-a-Go-Go (hERG) K+ Channels by Cultivation at Reduced Temperature. *BMC Biotechnol*. **2007**, *7*, 93.
13. Fryer, J. D.; Lukas, R. J. Noncompetitive Functional Inhibition at Diverse, Human Nicotinic Acetylcholine Receptor Subtypes by Bupropion, Phencyclidine, and Ibogaine. *J. Pharmacol. Exp. Ther*. **1999**, *288*, 88–92.
14. Papke, R. L.; Sanberg, P. R.; Shytle, R. D. Analysis of Mecamylamine Stereoisomers on Human Nicotinic Receptor Subtypes. *J. Pharmacol. Exp. Ther*. **2001**, *297*, 646–656.
15. Slemmer, J. E.; Martin, B. R.; Damaj, M. I. Bupropion Is a Nicotinic Antagonist. *J. Pharmacol. Exp. Ther*. **2000**, *295*, 321–327.
16. Zaveri, N.; Jiang, F.; Olsen, C.; et al. Novel Alpha3beta4 Nicotinic Acetylcholine Receptor-Selective Ligands. Discovery, Structure-Activity Studies, and Pharmacological Evaluation. *J. Med. Chem*. **2010**, *53*, 8187–8191.
17. Jepsen, T. H.; Jensen, A. A.; Lund, M. H.; et al. Synthesis and Pharmacological Evaluation of DHbetaE Analogues as Neuronal Nicotinic Acetylcholine Receptor Antagonists. *ACS Med. Chem. Lett*. **2014**, *5*, 766–770.
18. Absalom, N. L.; Quek, G.; Lewis, T. M.; et al. Covalent Trapping of Methyllycaconitine at the Alpha4-Alpha4 Interface of the Alpha4beta2 Nicotinic Acetylcholine Receptor: Antagonist Binding Site and Mode of Receptor Inhibition Revealed. *J. Biol. Chem*. **2013**, *288*, 26521–26532.
19. Liu, M.; Dilger, J. P. Site Selectivity of Competitive Antagonists for the Mouse Adult Muscle Nicotinic Acetylcholine Receptor. *Mol. Pharmacol*. **2009**, *75*, 166–173.
20. Arias, H. R.; Targowska-Duda, K. M.; Feuerbach, D.; et al. Different Interaction between Tricyclic Antidepressants and Mecamylamine with the Human Alpha3beta4 Nicotinic Acetylcholine Receptor Ion Channel. *Neurochem. Int*. **2010**, *56*, 642–649.
21. Arias, H. R.; Santamaria, A.; Ali, S. F. Pharmacological and Neurotoxicological Actions Mediated by Bupropion and Diethylpropion. *Int. Rev. Neurobiol*. **2009**, *88*, 223–255.
22. Ohtani, H.; Hanada, E.; Hirota, M.; et al. Inhibitory Effects of the Antihistamines Epinastine, Terfenadine, and Ebastine on Potassium Currents in Rat Ventricular Myocytes. *J. Pharm. Pharmacol*. **1999**, *51*, 1059–1063.
23. Takahashi, N.; Aizawa, H.; Inoue, H.; et al. Effects of Epinastine Hydrochloride on Cholinergic Neuro-Effector Transmission in Canine Tracheal Smooth Muscle. *Eur. J. Pharmacol*. **1998**, *358*, 55–61.
24. Berger, M. L.; Maciejewska, D.; Vanden Eynde, J. J.; et al. Pentamidine Analogs as Inhibitors of [(3)H]MK-801 and [(3)H]ifenprodil Binding to Rat Brain NMDA Receptors. *Bioorg. Med. Chem*. **2015**, *23*, 4489–4500.
25. Chen, X.; Qiu, L.; Li, M.; et al. Diarylamidines: High Potency Inhibitors of Acid-Sensing Ion Channels. *Neuropharmacology* **2010**, *58*, 1045–1053.
26. Sarashina, A.; Tatami, S.; Yamamura, N.; et al. Population Pharmacokinetics of Epinastine, a Histamine H1 Receptor Antagonist, in Adults and Children. *Br. J. Clin. Pharmacol*. **2005**, *59*, 43–53.
27. Ishiguro, N.; Nozawa, T.; Tsujihata, A.; et al. Influx and Efflux Transport of H1-Antagonist Epinastine across the Blood-Brain Barrier. *Drug Metab. Dispos*. **2004**, *32*, 519–524.
28. Wenzler, T.; Yang, S.; Braissant, O.; et al. Pharmacokinetics, *Trypanosoma brucei gambiense* Efficacy, and Time of Drug Action of DB829, a Preclinical Candidate for Treatment of Second-Stage Human African Trypanosomiasis. *Antimicrob. Agents Chemother*. **2013**, *57*, 5330–5343.
29. Sanderson, L.; Dogruel, M.; Rodgers, J.; et al. Pentamidine Movement across the Murine Blood-Brain and Blood-Cerebrospinal Fluid Barriers: Effect of Trypanosome Infection, Combination Therapy, P-Glycoprotein, and Multidrug Resistance-Associated Protein. *J. Pharmacol. Exp. Ther*. **2009**, *329*, 967–977.